Journal of Controlled Release 154 (2011) 42–49

Contents lists available at ScienceDirect

Journal of Controlled Release

journal homepage: www.elsevier.com/locate/jconrel

Localized ultrasound enhances delivery of rapamycin from microbubbles to prevent smooth muscle proliferation

Linsey C. Phillips [a], Alexander L. Klibanov [b], Brian R. Wamhoff [b,c,1], John A. Hossack [a,*,1]

[a] Department of Biomedical Engineering, University of Virginia, Charlottesville, VA, United States
[b] Department of Medicine, Cardiovascular Division, University of Virginia, Charlottesville, VA, United States
[c] Robert M. Berne Cardiovascular Research Center, University of Virginia, Charlottesville, VA, United States

ARTICLE INFO

Article history:
Received 15 November 2010
Accepted 17 April 2011
Available online 23 April 2011

Keywords:
Ultrasound contrast agents
Microbubbles
Drug delivery
Smooth muscle cells
Rapamycin

ABSTRACT

Microbubble contrast agents have been shown to enhance reagent delivery when activated by ultrasound. We hypothesized that ultrasound would enhance delivery of rapamycin, an antiproliferative agent, from the shell of microbubbles, thus reducing proliferation of vascular smooth muscle cells. Our objective was to determine optimal ultrasound parameters that maximized therapeutic efficacy, maintained cell adherence, and minimized the drug exposure time. *In vitro* assays determined that ultrasound (1 MHz, 0.5% duty cycle) is required to successfully deliver rapamycin from microbubbles and reduce proliferation. Co-injection of rapamycin with control microbubbles did not result in a reduction in proliferation. Successful reduction in proliferation (>50%) required pulses at least 10 cycles in length and at least 300 kPa peak negative pressure at which point 90% of cells remained adherent. The anti-proliferative effect was also localized within a 6 mm wide zone by focusing the ultrasound beam.

1. Introduction

Coronary heart disease, affecting 16.8 million Americans, is the result of fatty plaque buildup or atherosclerosis [1] in arteries. Angioplasty is the primary therapy for partially occluded atherosclerotic vessels. To prevent elastic recoil following angioplasty, metal stents are expanded against the vessel wall. Although these procedures alleviate vessel re-occlusion by providing a mechanical scaffold, they also cause injury to the vessel wall [2]. The injury induces proliferation of vascular smooth muscle cells, which over time can result in restenosis, a re-occlusion of the artery [3]. This process of hyperplasia is the main cause of in-stent restenosis [4]. Drug eluting stents (DES) reduce proliferation of adjacent cells, but are associated with an increased risk of late thrombosis or death [5,6]. Anti-platelet (*e.g.* Clopidogrel and/or Aspirin) therapy is therefore prescribed, often indefinitely, to these patients, leading to an increased risk of bleeding [7]. Moreover, restenting a restonic artery presents additional challenges. Due to these complications there has been an ongoing search for localized methods of anti-proliferative drug delivery to vessel walls following angioplasty.

Both rapamycin (sirolimus) and paclitaxel are drugs that have been incorporated into a DES. Rapamycin is a small molecule (MW = 914 g/mol) that is relatively insoluble in water [8] and acts both as an anti-inflammatory immunosuppressant and an anti-proliferative agent. Since it interrupts the cell cycle early in G1 phase it is considered to be cytostatic, and therefore less toxic than drugs which act later in the cycle such as paclitaxel [9,10]. Due to the potency of rapamycin, only a small amount is required to achieve an anti-proliferative effect [11]. *In vitro* studies have determined that a concentration of 10 ng/ml (2.5–14 nM) is sufficient to reduce vascular smooth muscle proliferation by 50% [9]. Furthermore, it is one of the most widely used agents on drug-eluting stents for the prevention of coronary artery restenosis [12].

The need for cardiovascular drug delivery agents has led to investigation of a variety of techniques including gene delivery, non-polymeric elution, and liposome agents. Microbubbles have also been under investigation as cardiovascular gene or drug delivery agents for several years [13–16]. Given that microbubbles are smaller than blood cells (generally 1–5 μm in diameter) they can safely traverse the entire vasculature. Commercial microbubble preparations (*e.g.* Definity) are stabilized by thin shells composed of protein (*e.g.* albumin), lipids, or polymers. Some commercial microbubbles are also US Food and Drug Administration approved for blood opacification. The microbubble shell can be modified to carry a drug payload [17,18], genes [19,20], or targeting ligands [18,20,21]. Additionally, microbubbles can enhance cell membrane permeability through a process known as sonoporation. Although the exact mechanism is not fully understood, the oscillation of the microbubble in an ultrasound field has been suggested to create transient pores in the lipid bilayer [22,23] and has also been attributed to microstreaming [24,25]. The formation of gas jets during microbubble rupture has also been proposed as a possible pore formation mechanism [26]. One group has

* Corresponding author at: Dept. of Biomedical Engineering, 415 Lane Road, MR5 Bldg., PO Box 800759, Charlottesville, VA 22908, United States. Tel.: +1 434 243 5866.
E-mail address: jh7fj@virginia.edu (J.A. Hossack).
[1] Authors contributed equally.

0168-3659/$ – see front matter © 2011 Elsevier B.V. All rights reserved.
doi:10.1016/j.jconrel.2011.04.020

suggested that the heavy perfluorocarbon gas contained in some experimental microbubble formulations may also be an enhancer of endothelial cell permeability [27]. Sonoporation is reversible, but can also lead to cell death under sufficiently high or long ultrasound exposure [24,28,29]. For example, Deng, Sieling, Pan, and Cui [29], observed an increased transmembrane current in cells subjected to both ultrasound and the presence of microbubbles indicating increased membrane porosity. Cells recovered back to resting levels in about 4 to 10 s following insonation for approximately 1 s at 1 MHz and 1 MPa pressure. Higher ultrasound intensities (>1 MPa), and longer durations (>0.5 s) resulted in irreversible cell damage and cell death. In view of these findings, the acoustic parameters must be carefully selected to achieve safe and effective localized delivery. Using conventional ultrasound focusing, microbubble induced effects can be limited to selected, focal regions. Previous studies have demonstrated localized reagent delivery to cells and tissues when microbubbles are placed in an ultrasound field [20,30,31].

To date, rapamycin has not been incorporated into lipid shelled microbubbles, only co-administered systemically [27]. In this paper, we report the use of rapamycin loaded microbubbles as an ultrasound-mediated, localized, drug delivery system to attenuate smooth muscle cell proliferation.

2. Methods

2.1. Cell culture

Optically and acoustically transparent [30,32], gas permeable, OptiCell™ (Biocrystal Inc., Westerville, OH) flasks, composed of 75 μm thick polystyrene membranes were coated with fibronectin (Invitrogen, Carlsbad, CA) for at least 4 h prior to plating the cells to ensure adherence. Primary rat aortic smooth muscle cells were plated at a density of 5×10^3 cells/cm^2 and incubated at 37 °C and 5% CO_2. They were cultured in growth (10% bovine serum) media (DMEM/F12, Gibco, Grand Island, NY) for 24 h where they reached 30–40% confluence.

2.2. Microbubble preparation and drug concentration determination

Due to the high solubility of rapamycin in lipids (tens of mg/ml), as compared to water (2–3 μg/ml) [8], rapamycin is an ideal candidate for incorporation into lipid-shelled microbubbles. Plain, control microbubbles were composed of base lipid components: phosphatidylcholine (2 mg/ml) (Avanti Lipids, Alabaster, AL) and polyethylene glycol stearate (2 mg/ml) (Sigma Chemical Co., St. Louis, MO). Rapamycin (0.4 mg/ml) (Chemwerth Inc., Woodbridge, CT) was added to the base lipids to produce drug-loaded microbubbles. The fluorescent dye, DiI (Molecular Probes, Eugene, OR) (trace amount), was added to the base lipids to produce fluorescent, control microbubbles. To generate lipid-shelled microbubbles an aqueous micellar dispersion of lipid and/or drug components was first generated by sonication for 5 min with an XL2020 sonicator (Misonix) equipped with a 1/2″ titanium probe, operated at 20 kHz and 50% maximum power. Once lipids were fully dispersed, a flow of decafluorobutane gas through a Teflon capillary immersed in the vial was started, and the vial was filled with decafluorobutane. Sonication of the vial was then performed for another 30 s at the maximum power setting of the XL2020 sonicator. During this procedure gas microbubbles were generated and became immediately coated and stabilized with the lipids present in the aqueous phase. After completion of the sonication procedure, this microbubble-stock vial was completely filled with decafluorobutane, sealed with a gastight screw-cap with a Teflon liner and stored at 4 °C.

Prior to running experiments each day, all microbubbles were separated from excess lipids and drug/dye by centrifugal flotation. Microbubble-stock was diluted into perfluorobutane-saturated phosphate buffered saline (Invitrogen, Carlsbad, CA) at a 1:2 ratio in a 3 ml syringe. The syringe was then spun in a centrifuge (Damon IEC HN-SII, IEC, Needham Heights, MA) at 1000 rpm, equivalent to 225×*g*, for 6 min to allow all the microbubbles to accumulate at the top of the syringe. The flotation process was repeated four times for every batch of microbubbles generated. The eluents from each flotation step were collected from four separate batches for further analysis. Concentration of the rapamycin or dye was analyzed from the eluent of each of the four flotations and from the final microbubble population (see Fig. 1). DiI concentration was measured on a relative fluorescence scale by a fluorescent plate reader (FLUOstar Omega, BMG Labtech, Offenburg, Germany). The DiI was excited at 544 nm and the emission at 590 nm was recorded. Rapamycin concentration was determined by HPLC analysis of reconstituted, lyophilized samples. For comparison, plain microbubbles were analyzed both by fluorescence and HPLC, neither of which registered any significant signal. The concentration of microbubbles was determined by electrozone sensing (Multisizer III, Beckman Coulter, Brea, CA). Regardless of the final concentration, washed microbubbles were diluted into Opticells such that the number of microbubbles injected was kept constant, not the amount of stock solution. For the control experiments, pure rapamycin was diluted to the same concentration found in the microbubbles.

2.3. Ultrasound conditions and experimental apparatus

Opticells were inverted so that cells were on the top side of the chamber. Opticells were inverted and submerged in a degassed water bath maintained at 37 °C. A neoprene absorber was placed below the Opticell at an angle of 30° to prevent standing wave formation. A focused (F = 42 mm), V302 1 MHz transducer (Olympus Panametrics, Waltham, MA) was positioned 42 mm above the Opticell chamber

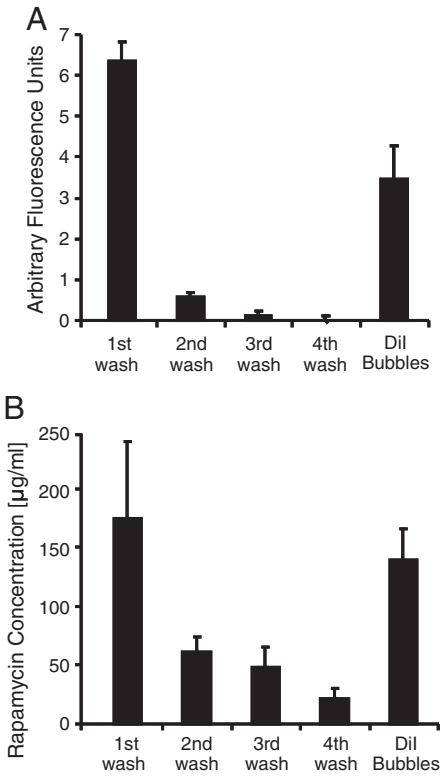

Fig. 1. Excess free dye (DiI) or drug (rapamycin) was removed during the washing procedure leaving ~21% of the rapamycin incorporated into the shell of the microbubbles. Microbubbles containing either rapamycin or DiI were washed four times by centrifugal flotation. The eluents were collected after each flotation and analyzed for fluorescence intensity (A — DiI microbubbles) or drug concentration by HPLC (B — rapamycin). Also analyzed was the final concentration in the microbubbles.

(Fig. 2) and was controlled using a linear motion stage (ESP3000, Newport Research Corp., Irvine, CA). For a wider beam width, the transducer was positioned closer to the Opticell (18 and 28 mm) thereby insonating a wider region of cells. For these three axial distances the peak negative pressure was adjusted to maintain a constant amplitude of 500 kPa at the location of the cells. Waveforms were supplied by an AWG2021 arbitrary wave generator (Tektronix, Beaverton, OR) and amplified by an A-500 60 dB RF power amplifier (ENI, Rochester, NY). The pulse repetition frequency (PRF) was set using a 5077PR pulser/receiver (Panametrics, Waltham, MA). All pulses were designed to be Gaussian with a 1 MHz center frequency and a 35% FWHM bandwidth. At an axial distance of 18 mm, the pulse length was varied between 1, 10, and 50 cycles per pulse and the duty cycle was kept constant (0.5%) by varying the PRF. The peak negative pressure amplitude was also varied between 0 and 800 kPa. A PVDF hydrophone (GL-0200, Onda Corp., Sunnyvale, CA) with a resolution of 0.5 mm, recorded the acoustic pressure along the width of the beam at the focal distance and two pre-focal axial distances (18 and 28 mm). Beam profiles of the ultrasound field were measured at each of the 3 distances over a width of 40 mm. The −6dB and −10 dB beam widths for each location are listed in Table 1.

Table 1
Measured acoustic beam widths and corresponding reduced proliferation widths.

Distance	18 mm	28 mm	42 mm
−6 dB width	11.0 mm	3.0 mm	2.5 mm
−10 dB width	12.5 mm	5.5 mm	3.5 mm
Anti-proliferation width	14 mm	8 mm	6 mm

The beam profiles were recorded using PVDF hydrophone at distances of 18, 28, and 42 mm from the transducer. The −6 dB and −10 dB beam widths are shown above. The corresponding width of the region of cells exhibiting a >50% decrease in proliferation are shown below each axial distance.

2.4. Drug delivery and proliferation assay

Opticells containing subconfluent layers of smooth muscle cells were injected with one of the following sets of reagents: rapamycin loaded microbubbles, rapamycin and separate DiI microbubbles, rapamycin alone, DiI microbubbles, or no microbubbles (equivalent volume of saline). Microbubbles were diluted in culture media such that the final injected concentration was 15×10^6 microbubbles/ml of media and contained approximately 95 mg/ml of rapamycin. The Opticells were immediately submerged in the water bath 2 min prior to insonation to allow the microbubbles to float toward the cells.

Initially, a 650 kPa ultrasound pulse with a 1 kHz PRF was applied for 9 min while the transducer was translated at a speed of 1 mm/s at a distance of 42 mm. This allowed for two 5×6 cm insonation regions and a control region in between to be produced within a single Opticell. Based on the beam width of this insonation configuration, each SMC received approximately 12.5 s of ultrasound which corresponds to ~12,500 pulses of ultrasound. Initially, Opticells were not washed following insonation, therefore the cells were exposed to the microbubbles and/or drug for the entire 48 hour incubation. In a second experiment, Opticells were washed with PBS 2 h after insonation to remove excess drug and microbubbles.

Cells were imaged under phase contrast microscopy at identified positions within the Opticell chambers at time zero (t0, less than 1 h after insonation and washing), at 24 h (t1) and at 48 h (t2) post-insonation. All non-adherent cells were removed during the washing step that immediately followed all 6-minute incubation experiments. Only whole, intact cells were counted at each time point. Proliferation was calculated as: $(Cells_{t1}-Cells_{t0})/Cells_{t0}$. The percent of cells adherent at t0 represents the total number of viable cells immediately following any microbubble or ultrasound treatment. By 48 h, control cells reached confluence and increases in proliferation were no longer discernable. Therefore, after this initial experiment, all proliferation measurements were made after 24 h, and unless otherwise noted, all proliferation rates are reported as the rate over 24 h.

To more closely mimic *in vivo* lifetime of drug delivery from microbubbles, the time in which the drug loaded microbubbles were inside the Opticell was shortened to 6 min, and the translation speed and PRF were increased to 2.5 mm/s and 5 kHz respectively. The total time in which cells were exposed to microbubbles or drug was thereby reduced to 6 min and the insonation time was reduced to 8.3 s per smooth muscle cell. Following insonation, Opticells were immediately washed with PBS to remove free drug/microbubbles and

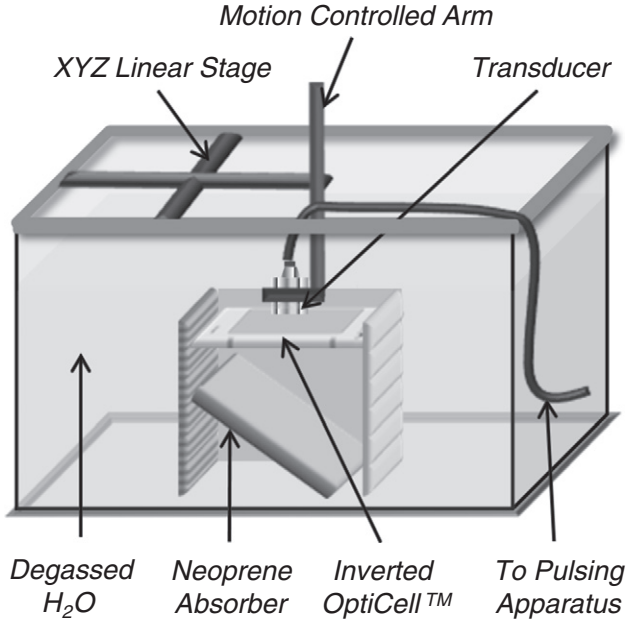

Fig. 2. Experimental apparatus. Rat aortic smooth muscle cells were plated in Opticell chambers which were then held in place in a 37 °C water bath using a plastic holder. An acoustic neoprene absorber was angled below the Opticell to reduce standing wave formation. A 1 MHz, V302 transducer, was positioned above the Opticell and controlled with a linear motion controller. Pulses were generated with an arbitrary waveform generator connected to a 60 dB amplifier. The PRF was set by an external pulser.

then refilled with growth media. Proliferation was again assessed, but only after 24 h. For each pulse length, the proliferation was assessed following insonation at 300 kPa and for each acoustic amplitude the proliferation was assessed after a pulse length of 10 cycles.

The ability of the drug delivery system to focus the anti-proliferative effect was also investigated. The beam width of the ultrasound field was widened as described in the previous section. Following application of a single line of ultrasound across the width of the Opticell, the cell proliferation was measured in 2 mm increments across the length of the Opticell. The transducer was positioned at 18, 28, and 42 mm from the cells thereby creating −6 dB beam widths of −11.0, 3.5, and 2.5 mm respectively. At each distance the spatial peak negative pressure at the location of the cells was maintained at 500 kPa by adjusting the input voltage to the amplifier.

2.5. Statistical analysis

A Student's *t*-test was used to determine statistical significance between groups. All experiments were conducted in at least triplicate. Where appropriate, ANOVA was used to determine significance among groups of three or more. A p value of less than 0.05 was considered significant.

3. Results

The concentration of microbubbles in the stock vial was between 2 and 3 billion per milliliter. After washing, the microbubbles were concentrated and stored at a concentration between 1 and 3 billion per milliliter. The average diameters of washed, prepared microbubbles were 2.6 μm, 2.5 μm, and 2.5 μm for plain, DiI, and rapamycin microbubbles respectively. As listed in Table 2, the standard deviations of all microbubbles from all batches of each type were very similar, and not statistically different from each other. In addition, all three types remained stable for at least 3 months when kept in their stock bottles under perfluorobutane headspace.

The measured fluorescence of the DiI microbubbles and their eluents from the flotation procedure follow a similar saturation pattern as compared to the eluents from HPLC analysis of the rapamycin microbubbles (see Fig. 1). Excess rapamycin or DiI which was not incorporated into the lipid shell was removed during centrifugal flotation. After 4 flotation washing steps, less than 6% of the rapamycin remained free in the final batch of rapamycin-loaded microbubbles. Similarly, less than 1% of the DiI remained free. These results indicate 20.6 ± 5.8% of the rapamycin was incorporated into the lipid shells. The final drug incorporation corresponds to approximately 4–8% of the total lipid shell, or 29 ng per million microbubbles. Degradation products of rapamycin, which were determined from HPLC-mass spectrometry described by Christians, Jacobsen, Serkova, Benet, Vidal, Sewing, Manns, and Kirchner [33,34], were not found in any of the samples, indicating that the process of forming the microbubbles does not degrade rapamycin.

Under our initial ultrasound conditions rapamycin loaded microbubbles significantly reduced proliferation of smooth muscle cells at both 24 and 48 h as compared to treatment with control microbubbles (Fig. 3). The cells were either not washed at all (48 hour incubation), or washed 2 h after insonation to remove the microbubbles and/or rapamycin. The decrease in proliferation after 48 h between cells treated with drug loaded and control microbubbles was significantly reduced 65% (Fig. 4). In Opticells washed 2 h after insonation, proliferation was significantly decreased by 55% by the combination of ultrasound and rapamycin microbubbles. After 2 h of incubation, free rapamycin also significantly reduced proliferation. In fact, when either rapamycin or rapamycin loaded microbubbles were incubated with cells for an extended period of time (at least 2 h), proliferation was reduced by at least 50% even without exposure to ultrasound.

Table 2
Microbubble size and variation of plain, DiI, or rapamycin microbubbles after the washing process.

MB type	Mean diameter ± S.D.
Plain	2.5 ± 1.5 μm
DiI	2.6 ± 1.4 μm
Rapamycin	2.5 ± 1.3 μm

For the remaining experiments, the total incubation time of the cells with microbubbles or drug was minimized and set to 6 min to more closely mimic acute *in vivo* conditions. Six minutes is the shortest time in which the experiment can accurately be repeated. Along with the shorter microbubble exposure time, the 1 MHz ultrasound pulses (Gaussian, 35% −6 dB bandwidth) were emitted at 650 kPa and 0.5% duty cycle for 8.3 s of insonation per smooth muscle cell. Only the cells left viable and adherent on the Opticell membrane were included in the initial count of cells. After insonation with either plain or rapamycin microbubbles, 25% of cells remained adherent, whereas 100% remained adherent when ultrasound was applied without any microbubbles (Fig. 5A). At the aforementioned acoustic amplitude and pulsing scheme the vehicle control (DiI microbubbles) did not affect proliferation (Fig. 5B). Additionally, under this shorter exposure period rapamycin microbubbles did not affect proliferation significantly unless insonated. Insonated cells which were exposed to rapamycin microbubbles for only 6 min incurred a 72% reduction in proliferation compared to vehicle controls (Fig. 5B). The combination of ultrasound and rapamycin-loaded microbubbles was necessary to achieve an anti-proliferative effect in a short period of time consistent with catheterization procedures in the clinical setting. The control microbubbles themselves did not affect proliferation with or without ultrasound. Similarly, applying 1 MHz, 50 cycle sinusoids at 500 kPa with 0.5% duty cycle for 8.3 s (Fig. 5C) reduced proliferation only in combination with the rapamycin loaded microbubbles. Free drug that was co-injected simultaneously with DiI microbubbles did not significantly reduce proliferation (Fig. 5C). Although drug concentration was kept constant, only the microbubbles which contained the drug in their shells significantly reduced proliferation (Fig. 5C).

Peak negative acoustic pressure and pulse length both affected drug delivery and proliferation of smooth muscle cells. With increasing pressure the proliferation rate decreased (Fig. 6A). For these experiments, the pulse length was kept constant at 10 cycles/pulse. Only beyond 300 kPa at 10 cycles per pulse was proliferation significantly decreased (Fig. 6A) indicating a threshold for drug delivery. The number of adherent cells also decreased with increasing peak negative pressure (Fig. 6C). For example, at 200, 300 and 400 kPa (PNP) the percents of viable, adherent cells were 176.4%, 55.2%, and 34.9% respectively. The corresponding reduction in proliferation was 9.3%, 27.9%, and 48.1% following insonation at 200, 300, and 400 kPa (PNP).

In a separate set of experiments the peak negative pressure was kept constant at 300 kPa. As the pulse length was increased from 1 to 10 to 50 cycles per pulse the proliferation rate also decreased (Fig. 6B). By reducing the number of cycles down to one, the delivery does not result in a reduction in proliferation, but with 10 cycles the reduction in proliferation was reduced by ~65% with approximately 55% adherence of the cells. Cells in Opticells which were not insonated were imaged for comparison. The proliferation rates of these cells remained constant. Some variation in basal proliferation rates existed between experiments due to the variation in passage time of the cells.

By decreasing the beam width of the applied ultrasound field the area of affected cells was narrowed to within 6 mm (Fig. 7). Cell proliferation was measured as a function of distance across the Opticell. The proliferation map was correlated to the beam width. The width of the region of cells exhibiting more than 50% reduction in

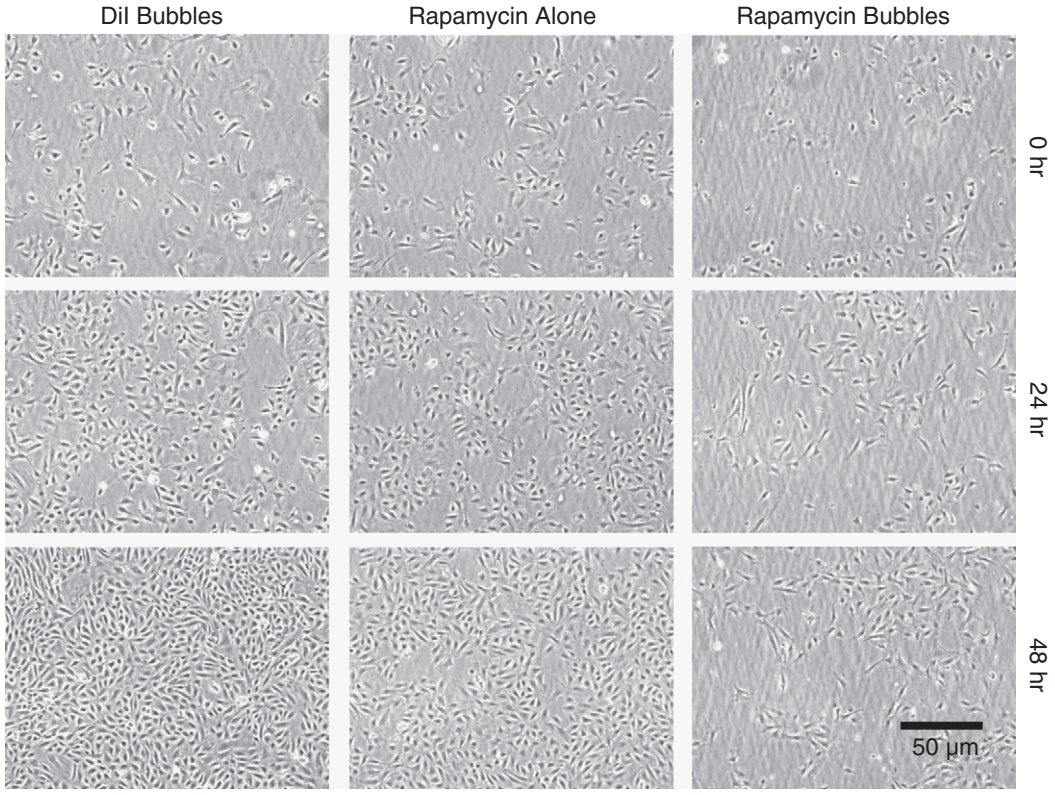

Fig. 3. Phase contrast images of smooth muscle cells following insonation (0 h), and both 24 and 48 hours later. Cells were incubated with one of the following: DiI microbubbles (vehicle control), free rapamycin, or rapamycin microbubbles (drug concentration matched in final dilution of 0.15×10^9 microbubbles). Free drug or microbubbles were not washed from the Opticell following insonation, and were therefore exposed to the cells for the full 48 hour period.

proliferation compared to surrounding, non-affected cells was measured for each variation of the ultrasound beam (Table 1). For the transducer positions corresponding to −20 dB beam widths of 15.0 mm, 7.5 mm, and 4.5 mm, the effective anti-proliferation regions were 14 mm, 8 mm, and 6 mm wide respectively.

4. Discussion and conclusions

We have demonstrated enhanced drug delivery to and reduced proliferation of smooth muscle cells *in vitro* following ultrasound-mediated rupture of rapamycin microbubbles. Initial studies indicated that rapamycin-loaded microbubbles reduced SMC proliferation by up to 65%, similar to the reduction induced by the dissolved rapamycin alone (52%). An estimated half life of lipid-shelled microbubbles in an artery *in vivo* is on the order of minutes. Under delivery and insonation times on the order of minutes, our chosen ultrasound treatment induced a significant anti-proliferative effect on the cells (72% reduction in proliferation compared to no microbubbles or ultrasound). In fact, without ultrasound, no significant drug delivery effect was detected indicating that the rapamycin microbubbles alone were not capable of reducing proliferation under our short exposure experimental conditions. If translated to an *in vivo* setting, a 72% reduction of smooth muscle cell proliferation could reduce neointima formation, as suggested by Parry, Brosius, Thyagarajan, Carter, Argentieri, Falotico, Siekierka [9].

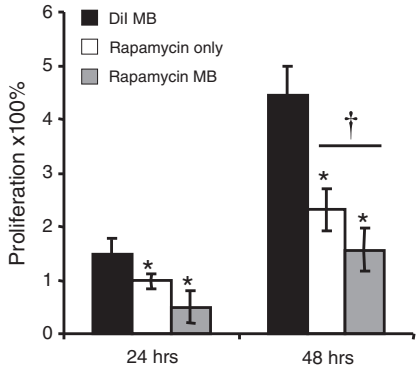

Fig. 4. Proliferation of smooth muscle cells after 24 and 48 hours after insonation (1 MHz, 600 kPa, 1 kHz PRF, Gaussian pulses) combined with DiI microbubbles, rapamycin alone, or rapamycin loaded microbubbles. Proliferation is measured as the percent increase in cell density. Free drug/microbubbles were incubated with cells for the full 48 hour period. *Statistical significance compared to DiI MB, †statistical significance compared to rapamycin only ($n \geq 4$, $p < 0.05$).

Control or DiI microbubbles also induced no reduction in proliferation regardless of ultrasound exposure. As we expected, ultrasound with control microbubbles did not significantly affect the proliferation of cells as long as no drug was present. All three types of microbubbles investigated caused equivalent numbers of cells to be dislodged from the Opticell membrane following insonation. Although many cells were knocked off following insonation, only cells remaining on the membrane were included in the count for baseline cell density at time zero. Given that no difference in proliferation was observed between groups treated with control microbubbles, or no microbubbles with or without ultrasound we conclude that the chosen ultrasound conditions were not killing a significant number of cells. One of the goals of this study was to apply ultrasound treatment which permeabilized cells without killing them. Although a molecular assay of viability was not performed, our results suggest that under the acoustic conditions investigated, cells adherent to the Opticell membrane are viable.

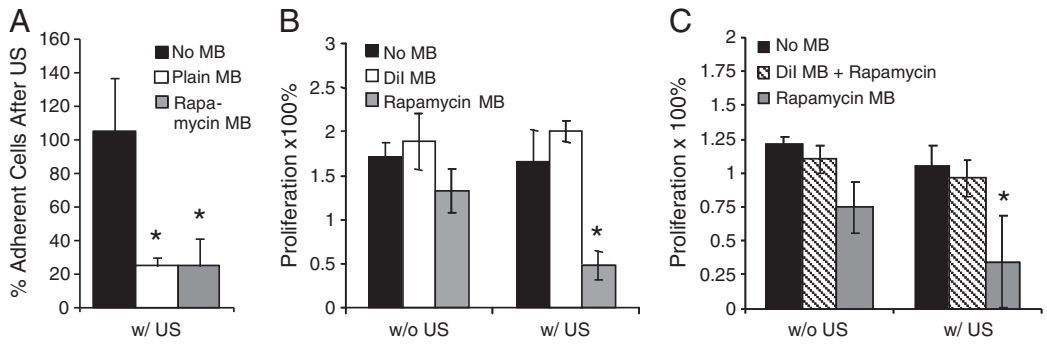

Fig. 5. The combination of ultrasound and rapamycin microbubbles (MB) is required for attenuation of SMC proliferation. A) Adherence of cells measured immediately following insonation with or without microbubbles. B) Cells were exposed to either no ultrasound (left) or ultrasound (1 MHz, single cycle, 650 kPa, 0.5% duty cycle, 8.3 s) without microbubbles, or with either control DiI microbubbles or rapamycin microbubbles. Cell proliferation, as measured by cell density at 0 and 24 hour post-insonation was decreased by 72% following ultrasound and rapamycin microbubble exposure. C) Cells were insonated (1 MHz, 50 cycle, 500 kPa, 0.5% duty cycle, 8.3 s), while exposed to either no microbubbles, DiI bubbles in combination with rapamycin, or rapamycin microbubbles. The rapamycin microbubbles and combined DiI microbubbles with rapamycin reduced proliferation by 71% and 21% respectively as compared to the untreated control. * Denotes statistical significance from other microbubble treatments, ($n \geq 4$, $p < 0.05$).

As peak negative pressure or pulse length was increased the proliferation of smooth muscle cells was decreased. This is believed to be due to an increased oscillatory motion of the microbubbles with increasing peak negative pressure. Fragmentation or rupture of the microbubbles has also previously been shown to enhance reagent delivery to cells [32,35]. A high speed camera was not incorporated into this work, so exactly when the microbubbles ruptured cannot be known. Based on the work by Chomas, Dayton, Morgan, Allen, and Ferrara [36,37], these lipid shelled rapamycin microbubbles are believed to rupture at 300 kPa or more. Since an increase in therapeutic effect was observed with increasing pulse length it is hypothesized that increased oscillation of the microbubble or free gas continues to enhance sonoporation and drug delivery into the cells. In order to reduce proliferation by at least 50%, a peak negative pressure of 400 kPa and a pulse length of more than 10 cycles were required. The optimal acoustic pulsing parameters for rapamycin delivery are around 400 kPa and at least 10 cycles in length. Duty cycle and frequency may also affect delivery, but were not investigated in this study.

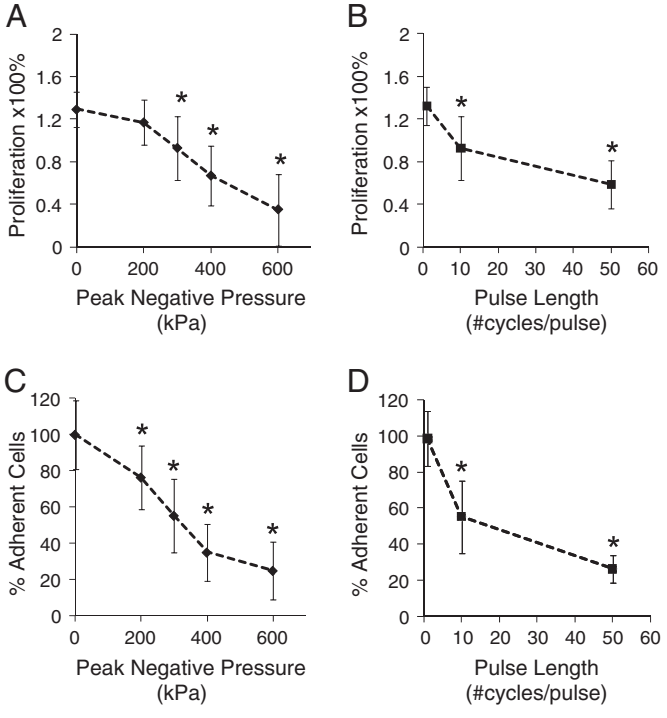

Fig. 6. Acoustic intensity and pulse length effects on rapamycin delivery from microbubbles. Proliferation of SMCs (A, B) and percentage of remaining adherent SMCs (C,D) following insonation with rapamycin microbubbles are plotted against peak negative pressure and pulse length. A, C) Ultrasound pulses 10 cycles in length were applied with increasing acoustic intensity. B,D) Ultrasound pulses at 300 kPa peak negative pressure were applied with varying pulse lengths and PRFs to maintain a constant duty cycle of 0.5%. (Expressed at mean ± S.D., $n \geq 4$, * denotes $p < 0.05$).

There is a trend toward reduced proliferation with the rapamycin microbubbles even without ultrasound because the drug is concentrated in the shell of the microbubbles. The microbubbles float up to the cells during the 6 minute experiments causing a higher concentration of rapamycin to accumulate near the cell surface than would happen during exposure to free rapamycin. So, although the concentration of rapamycin injected into each Opticell was kept constant across experiments, the amount of drug in very close proximity to the cells is different when injecting it separately from microbubbles. These results demonstrate the advantage of using drug-loaded microbubbles over free drug with microbubbles. Although this rapamycin-delivery technology has not yet been transferred to an *in vivo* model, the addition of ultrasound may allow for enhanced membrane permeability *in vivo*, leading to greater drug delivery into localized tissues of interest. In fact, we can reasonably expect an enhancement given that we have already reported localized gene delivery in a porcine model of coronary artery injury *in vivo* using microbubbles and intravascular ultrasound [31]. Furthermore, our microbubbles may also be targeted to molecular markers such as VCAM-1. These targeted microbubbles resulted in enhanced gene transfection under localized ultrasound application [38]. Importantly, when ultrasound mediated delivery is applied to smooth muscle cells, rapamycin does not need to be present for an extended period of time to reduce proliferation, as was the case without ultrasound. This result suggests that prolonged exposure is not necessary.

Rapamycin has been applied in conjunction with nanoparticle emulsions and perfluorocarbon albumin microbubbles with some success, but has not been incorporated into the shell of the microbubbles. In a porcine model of restenosis, rapamycin was incorporated with molecular-targeted ($\alpha_v\beta_3$) nanoparticles with perfluorocarbon cores [39]. In order to allow "contact facilitated drug delivery" the arteries in rabbits were clamped off for more than 5 min. No ultrasound was applied. In the clinical setting, obstruction of blood flow to major arteries such as the coronaries could lead to subsequent harm, including myocardial infarction, far outweighing the benefit of contact facilitated rapamycin delivery. In another study, systemic delivery of albumin microbubbles and rapamycin were injected intravenously into two pigs which had undergone stent

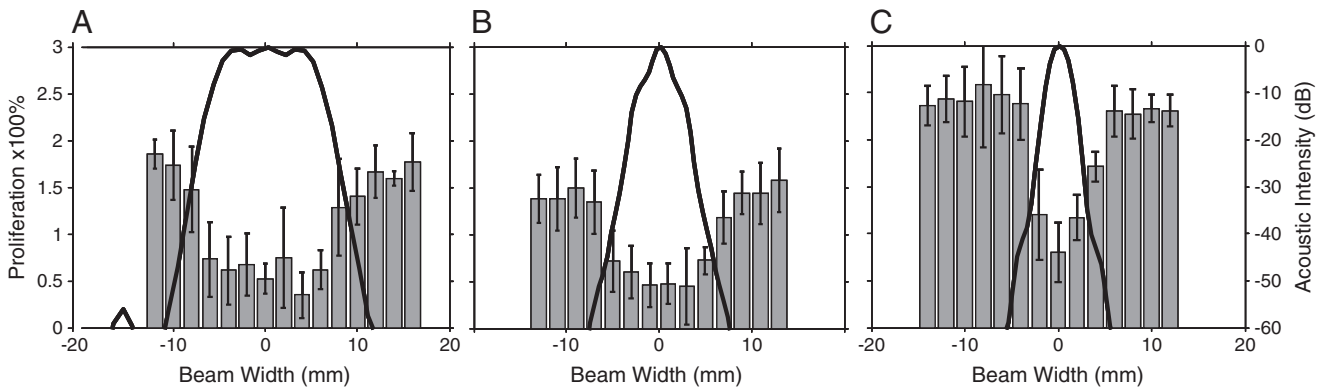

Fig. 7. Focusing the ultrasound beam results in focal delivery of rapamycin and localized reduction in proliferation. Rapamycin microbubbles were infused with smooth muscle cells prior to insonation. The acoustic output of the V302 transducer at distances of A) 18, B) 28, and C) 42 mm, as measured by a PVDF hydrophone, is overlaid on proliferation maps (gray bars) of smooth muscle cells *in vitro*. Proliferation was measured across 2 mm regions of cells. Peak negative pressure at the location of the cells was maintained at 500 kPa regardless of the axial location of the transducer. The ultrasound beam intensity is plotted in decibels.

implantation [27]. Again, no ultrasound was applied. A decrease in neointimal formation was observed in these two pigs, however the loading dose was high (2 mg). An injection of 2 mg of rapamycin in the blood is consistent with side effects in humans [40]. In a different study with equally sized pigs, 4 to 8 times less rapamycin was injected intramuscularly [41]. Loading rapamycin into the shell of microbubbles, locally delivering them through a catheter (as described previously [31]), and rupturing them with ultrasound at the site of vessel injury allows for treatment with a much lower total drug dose. Another advantage of ultrasound mediated delivery is the short period of time (on the order of seconds) needed to deliver the drug. Obstruction of blood flow will not be necessary with the proposed method of ultrasound mediated rapamycin delivery from microbubbles if combined with high intensity intravascular ultrasound or focused transcutaneous ultrasound. We recently confirmed that intravascular ultrasound (2 MPa) can deliver plasmid DNA from microbubbles to a pig coronary artery under flow [31].

Future studies could incorporate molecular targeting ligands to receptors such as VCAM-1 or $\alpha_v\beta_3$. In addition, radiation force ultrasound could be applied to locally "push" microbubbles against the vessel wall. Microbubbles in the 1–5 um range, like ours, are well suited for pushing and imaging. Smaller microbubbles (<500 nm) lack sufficient echogenicity [42] and travel much shorter distances under radiation force [43]. Using both radiation force and molecular targeting offers the potential to further enhance the delivery of therapeutic reagents. Shorter insonation time, or a more highly focused transducer may be capable of inducing drug delivery on narrower regions of interest.

Our research supports the contention that ultrasound mediated rapamycin delivery from lipid shelled microbubbles might be developed to preventatively treat stented or injured arteries. A modified intravascular ultrasound catheter would allow for site specific imaging and drug delivery along the vessel lumen. This technology could theoretically be applied immediately following surgery, while the patient already has a catheter in place. The rapamycin delivery system proposed herein will need to be tested *in vivo*, but has already demonstrated promise for localized prevention of smooth muscle cell proliferation.

Acknowledgments

This work was supported in part by National Institutes of Health NIBIB grant# EB002185 to ALK, JAH and NHLBI HL090700 to BRW, ALK, JAH, UVA Coulter Translational Research Grant to BRW, ALK, JAH and an American Heart Association Graduate Fellowship to LCP.

The authors would also like to thank Pam Schoppee-Bortz, Oana Nicara, and Themistoclis Karaoli for their aid in cell culture, and Lauren Wahl for aid in cell image analysis.

References

[1] V.L. Roger, A.S. Go, D.M. Lloyd-Jones, R.J. Adams, J.D. Berry, T.M. Brown, M.R. Camethon, S. Dai, G. de Simone, E.S. Ford, C.S. Fox, H.J. Fullerton, C. Gillespie, K.J. Greenlund, S.M. Hailpem, J.A. Heit, P.M. Ho, V.J. Howard, B.M. Kissela, S.J. Kittner, D.T. Lackland, J.H. Lichtman, L.D. Lisabeth, D.M. Makuc, G.M. Marcus, A. Marelli, D.B. Matchar, M.M. McDermott, J.B. Meigs, C.S. Moy, D. Mozaffarian, M.E. Mussolino, G. Nichol, N.P. Paynter, W.D. Rosamond, P.D. Sorlie, R.S. Stafford, T.N. Turan, M.B. Turner, N.D. Wong, J. Wylie-Rosett, A.H.A.S. Comm, S. Stroke Stat, Heart disease and stroke statistics — 2011 update a report from the American Heart Association, Circulation 123 (2011) E18–E209.
[2] P.H. Grewe, T. Deneke, A. Machraoui, J. Barmeyer, K.M. Muller, Acute and chronic tissue response to coronary stent implantation: pathologic findings in human specimen, J. Am. Coll. Cardiol. 35 (2000) 157–163.
[3] R.S. Schwartz, Pathophysiology of restenosis: interaction of thrombosis, hyperplasia and/or remodeling, Am. J. Cardiol. 81 (1998) 14E–17E.
[4] R. Kornowski, M.K. Hong, F.O. Tio, O. Bramwell, H.S. Wu, M.B. Leon, In-stent restenosis: contributions of inflammatory responses and arterial injury to neointimal hyperplasia, J. Am. Coll. Cardiol. 31 (1998) 224–230.
[5] R.A. Byrne, N. Sarafoff, A. Kastrati, A. Schomig, Drug-eluting stents in percutaneous coronary intervention: a benefit –risk assessment, Drug Saf. 32 (2009) 749–770.
[6] E. Camenzind, P.G. Steg, W. Wijns, Stent thrombosis late after implantation of first-generation drug-eluting stents — a cause for concern, Circulation 115 (2007) 1440–1455.
[7] E.L. Eisenstein, K.J. Anstrom, D.F. Kong, L.K. Shaw, R.H. Tuttle, D.B. Mark, J.M. Kramer, R.A. Harrington, D.B. Matchar, D.E. Kandzari, E.D. Peterson, K.A. Schulman, R.M. Califf, Clopidogrel use and long-term clinical outcomes after drug-eluting stent implantation, JAMA 297 (2007) 159–168.
[8] P. Simamora, J.M. Alvarez, S.H. Yalkowsky, Solubilization of rapamycin, Int. J. Pharm. 213 (2001) 25–29.
[9] T.J. Parry, R. Brosius, R. Thyagarajan, D. Carter, D. Argentieri, R. Falotico, J. Siekierka, Drug-eluting stents: sirolimus and paclitaxel differentially affect cultured cells and injured arteries, Eur. J. Pharmacol. 524 (2005) 19–29.
[10] R. Wessely, A. Schomig, A. Kastrati, Sirolimus and paclitaxel on polymer-based drug-eluting stents — similar but different, J. Am. Coll. Cardiol. 47 (2006) 708–714.
[11] S.O. Marx, T. Jayaraman, L.O. Go, A.R. Marks, Rapmaycin-FKBP inhibits cell-cycle regulators of proliferation in vascular smooth-muscle cells, Circ. Res. 76 (1995) 412–417.
[12] J.M. Siller-Matula, I. Tentzeris, B. Vogel, S. Schacherl, R. Jarai, A. Geppert, G. Unger, K. Huber, Tacrolimus-eluting carbon-coated stents *versus* sirolimus-eluting stents for prevention of symptom-driven clinical end points, Clin. Res. Cardiol. 99 (2010) 645–650.
[13] K. Ferrara, R. Pollard, M. Bordeni, Ultrasound microbubble contrast agents: fundamentals and application to gene and drug delivery, Annu. Rev. Biomed. Eng. 9 (2007) 415–447.
[14] E.C. Unger, E. Hersh, M. Vannan, T.O. Matsunaga, M. McCreery, Local drug and gene delivery through microbubbles, Prog. Cardiovasc. Dis. 44 (2001) 45–54.
[15] E.C. Unger, T. Porter, W. Culp, R. Labell, T. Matsunaga, R. Zutshi, Therapeutic applications of lipid-coated microbubbles, Adv. Drug Deliv. Rev. 56 (2004) 1291–1314.
[16] R. Bekeredjian, P.A. Grayburn, R.V. Shohet, Use of ultrasound contrast agents for gene or drug delivery in cardiovascular medicine, J. Am. Coll. Cardiol. 45 (2005) 329–335.

[17] J.A. Kang, X.L. Wu, Z.G. Wang, H.T. Ran, C.S. Xu, J.F. Wu, Z.X. Wang, Y. Zhang, Antitumor effect of docetaxel-loaded lipid microbubbles combined with ultrasound-targeted microbubble activation on VX2 rabbit liver tumors, J. Ultrasound Med. 29 (2010) 61–70.
[18] M.S. Tartis, J. McCallan, A.F.H. Lum, R. LaBell, S.M. Stieger, T.O. Matsunaga, K.W. Ferrara, Therapeutic effects of paclitaxel-containing ultrasound contrast agents, Ultrasound Med. Biol. 32 (2006) 1771–1780.
[19] M. Vannan, T. McCreery, P. Li, Z.G. Han, E. Unger, B. Kuersten, E. Nabel, S. Rajagopalan, Ultrasound-mediated transfection of canine myocardium by intravenous administration of cationic microbubble-linked plasmid DNA, J. Am. Soc. Echocardiogr. 15 (2002) 214–218.
[20] J.P. Christiansen, B.A. French, A.L. Klibanov, S. Kaul, J.R. Lindner, Targeted tissue transfection with ultrasound destruction of plasmid-bearing cationic microbubbles, Ultrasound Med. Biol. 29 (2003) 1759–1767.
[21] E.A. Ferrante, J.E. Pickard, J. Rychak, A. Klibanov, K. Ley, Dual targeting improves microbubble contrast agent adhesion to VCAM-1 and P-selectin under flow, J. Control. Release 140 (2009) 100–107.
[22] A. van Wamel, K. Kooiman, M. Harteveld, M. Emmer, F.J. ten Cate, M. Versluis, N. de Jong, Vibrating microbubbles poking individual cells: drug transfer into cells via sonoporation, J. Control. Release 112 (2006) 149–155.
[23] B.D.M. Meijering, L.J.M. Juffermans, A. van Wamel, R.H. Henning, I.S. Zuhorn, M. Emmer, A.M.G. Versteilen, W.J. Paulus, W.H. van Gilst, K. Kooiman, N. de Jong, R.J.P. Musters, L.E. Deelman, O. Kamp, Ultrasound and microbubble-targeted delivery of macromolecules is regulated by induction of endocytosis and pore formation, Circ. Res. 104 (2009) 679–687.
[24] J.R. Wu, J.P. Ross, J.F. Chiu, Reparable sonoporation generated by microstreaming, J. Acoust. Soc. Am. 111 (2002) 1460–1464.
[25] J. Collis, R. Manasseh, P. Liovic, P. Tho, A. Ooi, K. Petkovic-Duran, Y.G. Zhu, Cavitation microstreaming and stress fields created by microbubbles, Ultrasonics 50 (2010) 273–279.
[26] M. Postema, A. Van Wamel, C.T. Lancee, N. De Jong, Ultrasound-induced encapsulated microbubble phenomena, Ultrasound Med. Biol. 30 (2004) 827–840.
[27] N.N. Kipshidze, T.R. Porter, G. Dangas, H. Yazdi, F. Tio, F. Xie, D. Hellinga, R. Wolfram, R. Seabron, R. Waksman, A. Abizaid, G. Roubin, S. Iyer, A. Colombo, M.B. Leon, J.W. Moses, P. Iversen, Novel site-specific systemic delivery of rapamycin with perfluorobutane gas microbubble carrier reduced neointimal formation in a porcine coronary restenosis model, Catheter. Cardiovasc. Interv. 64 (2005) 389–394.
[28] R. Karshafian, P.D. Bevan, R. Williams, S. Samac, P.N. Burns, Sonoporation by ultrasound-activated microbubble contrast agents: effect of acoustic exposure parameters on cell membrane permeability and cell viability, Ultrasound Med. Biol. 35 (2009) 847–860.
[29] C.X. Deng, F. Sieling, H. Pan, J.M. Cui, Ultrasound-induced cell membrane porosity, Ultrasound Med. Biol. 30 (2004) 519–526.
[30] A. Rahim, S.L. Taylor, N.L. Bush, G.R. Ter Haar, J.C. Bamber, C.D. Porter, Physical parameters affecting ultrasound/microbubble-mediated gene delivery efficiency *in vitro*, Ultrasound Med. Biol. 32 (2006) 1269–1279.
[31] L.C. Phillips, A.L. Klibanov, D.K. Bowles, M. Ragosta, J.A. Hossack, B.R. Wamhoff, Focused *in vivo* delivery of plasmid dna to the porcine vascular wall via intravascular ultrasound destruction of microbubbles, J. Vasc. Res. 47 (2010) 270–274.
[32] D.L. Miller, C.Y. Dou, J.M. Song, DNA transfer and cell killing in epidermoid cells by diagnostic ultrasound activation of contrast agent gas bodies *in vitro*, Ultrasound Med. Biol. 29 (2003) 601–607.
[33] U. Christians, W. Jacobsen, N. Serkova, L.Z. Benet, C. Vidal, K.F. Sewing, M.P. Manns, G.I. Kirchner, Automated, fast and sensitive quantification of drugs in blood by liquid chromatography–mass spectrometry with on-line extraction: immunosuppressants, J. Chromatogr. B Analyt. Technol. Biomed. Life Sci. 748 (2000) 41–53.
[34] Y.L. Zhang, J. Bendrick-Peart, T. Strom, M. Haschke, U. Christians, Development and validation of a high-throughput assay for quantification of the proliferation inhibitor ABT-578 using LC/LC-MS/MS in blood and tissue samples, Ther. Drug Monit. 27 (2005) 770–778.
[35] H. Pan, Y. Zhou, O. Izadnegahdar, J.M. Cui, C.X. Deng, Study of sonoporation dynamics affected by ultrasound duty cycle, Ultrasound Med. Biol. 31 (2005) 849–856.
[36] J. Chomas, P. Dayton, K. Morgan, J. Allen, K. Ferrara, Optimization of microbubble destruction, Proc. IEEE Ultrason. Symp. 2 (1999) 1689–1692.
[37] J.E. Chomas, P. Dayton, J. Allen, K. Morgan, K.W. Ferrara, Mechanisms of contrast agent destruction, IEEE Trans. Ultrason. Ferroelectr. Freq. Control 48 (2001) 232–248.
[38] L.C. Phillips, A.L. Klibanov, B.R. Wamhoff, J.A. Hossack, Intravascular ultrasound detection and delivery of molecularly targeted microbubbles for gene delivery, Proc. IEEE Ultrason. Symp. 1 (2009) 1–4.
[39] T. Cyrus, H.Y. Zhang, J.S. Allen, T.A. Williams, G. Hu, S.D. Caruthers, S.A. Wickline, G.M. Lanza, Intramural delivery of rapamycin with alpha(v)beta(3)-targeted paramagnetic nanoparticles inhibits stenosis after balloon injury, Arterioscler. Thromb. Vasc. Biol. 28 (2008) 820–826.
[40] K. Mahalati, B.D. Kahan, Clinical pharmacokinetics of sirolimus, Clin. Pharmacokinet. 40 (2001) 573–585.
[41] R. Gallo, A. Padurean, T. Jayaraman, S. Marx, M. Rogue, S. Adelman, J. Chesebro, J. Fallon, V. Fuster, A. Marks, J.J. Badimon, Inhibition of intimal thickening after balloon angioplasty in porcine coronary arteries by targeting regulators of the cell cycle, Circulation 99 (1999) 2164–2170.
[42] A.L. Klibanov, P.T. Rasche, M.S. Hughes, J.K. Wojdyla, K.P. Galen, J.H. Wible, G.H. Brandenburger, Detection of individual microbubbles of an ultrasound contrast agent: fundamental and pulse inversion imaging, Acad. Radiol. 9 (2002) S279–S281.
[43] P.A. Dayton, J.S. Allen, K.W. Ferrara, The magnitude of radiation force on ultrasound contrast agents, J. Acoust. Soc. Am. 112 (2002) 2183–2192.